Gas Dispersion in Downflowing High Velocity Fluidized Beds

Chunshe Cao and Herbert Weinstein
Dept. of Chemical Engineering, The City College of New York, New York, NY 10031

Measurements are presented of gas mixing in a downflowing high-velocity fluidized bed using helium tracer detected by an on-line analyzer. It was found that gas backmixing is very limited in the downer, and the lateral mixing is comparable with that in the riser. A dispersion model is applied to characterize the behavior of the gas mixing in the two-phase downflowing mixture.

Introduction

The gas-solid cocurrent downflowing high-velocity fluidized bed (downer) is under investigation for very short residence-time industrial applications, such as advanced thermal cracking and catalytic cracking of hydrocarbons (Gartside, 1989; Murphy, 1992). The efficiency of a downer reactor depends on its ability to mix adequately the incoming flows of reactants with the solids, and performance criteria such as yield and selectivity are typically adversely affected by backmixing in short contact time or residence time processes. As unit residence-time requirements become shorter, the backmixing inherent in the upflow riser system becomes more critical in limiting process yields and selectivity. A low gas backmixing level has been expected in proposals for the development of the downer reactor.

Flow patterns in the downer (Cao, 1998) show solids aggregation, nonuniform radial gas and solids velocity distributions and relatively uniform axial solids concentration profiles, which are different from those in the riser. This indicates that there is a significant difference in gas mixing behavior between the downer and the riser, and independent downer measurements are required. However, a sufficient database for high-velocity downflow gas mixing properties of gas-solid powder mixtures upon which a process development can be based is not available. Thus, a clear understanding of gas lateral dispersion and backmixing in the downer is important. In this investigation, a helium tracing technique (Weinstein et al., 1989) is used to provide a picture of gas intermixing and backmixing in the high velocity gas-solid downflowing mixture.

Correspondence concerning this article should be addressed to H. Weinstein.
Current address of C. Cao: Exxon Mobil Research and Engineering Company, Clinton, Township, Annandale, NJ 08801.

Experimental Studies

This investigation was conducted in the City College downer-riser circulating fluidized bed (Cao, 1998), which incorporates a downer, a return riser, a storage tank, a solid feed device, and a gas-solids separation system. The system is shown in Figure 1. The downer is made of a Plexiglas tube with an inner diameter of 12.7 cm and a length of 4.6 m. The bed material used for the entire investigation was Grace Davison fluid cracking catalyst, which has a particle density of 1,480 kg/m^3 and mean diameter of 82 μm. A solid feeder and a gas distributor are located on top of the downer in a wye arrangement. A hand operated valve is located between the storage tank and the solid feeder to control the solid flow rate. The solids are carried down by the main air supply to a U-bend section, which connects the downer with the return riser. The fluidizing medium is ambient air. Additional air enters the system in the U-bend section regulated separately through four independent air supply lines with five nozzles. It helps to carry up the solids through the riser. The riser is also made of Plexiglas with a height of 8.85 m and with the same diameter as that of the downer. The solid particles are carried up through the riser, which terminates in a flexible nylon tube, and are directed into the primary cyclone. The primary cyclone is located in the top of the storage tank. The Plexiglas vessel (0.3048 m in ID; wall thickness 1.27 cm) is used as a storage bed for the solid. The solids separated in the primary cyclone fall down along the wall of the storage bed, which is kept at bubbling fluidization conditions. After passing through the secondary cyclone (Fisher-Klosterman Cyclone Collector), the air is exhausted through a bag filter which collects the fines. The fines collected are returned periodically to the system. The separated solids from the secondary cyclone return to the storage tank by a standpipe. The

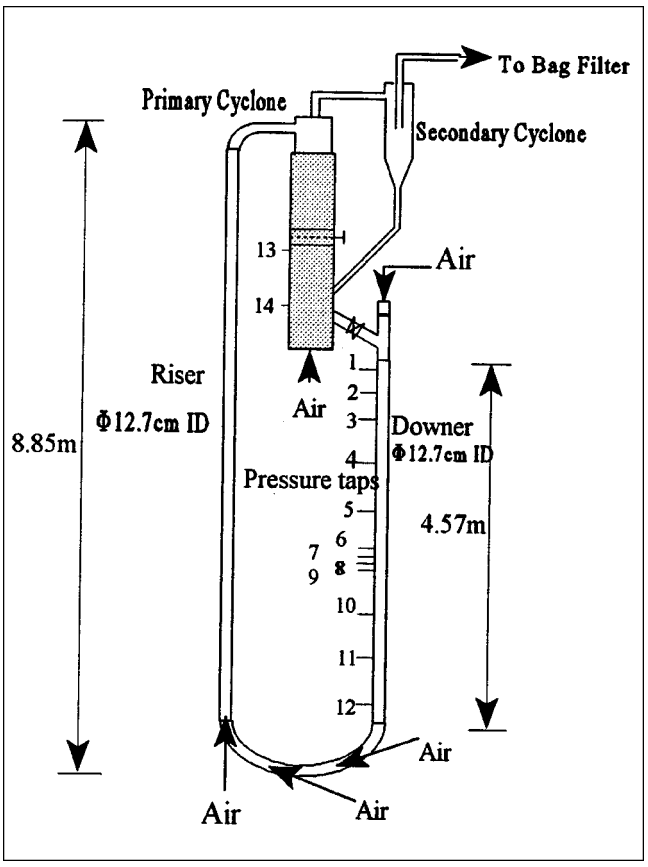

Figure 1. Downer-riser circulating fluidization unit.

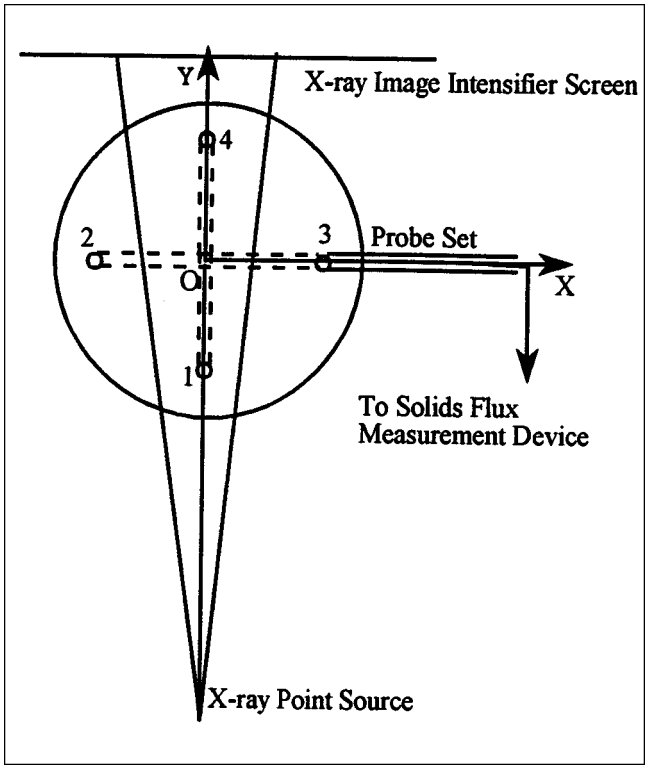

Figure 2. Cross-section of the downer with the solids downflow flux measurement probe set.

butterfly valve in the middle of the storage bed is made out of a sintered plate. It is used to measure the solid flow rate (Schnitzlein and Weinstein, 1988).

Measurements of radial solid density with an X-ray imaging technique indicate that solids distribution in the downer is asymmetric in the *r*-direction within the solids entrance region, and become symmetric about 1.2 m below the solids inlet (Cao, 1998). To verify the existence of axial symmetry below 1.2 m, a set of flux probes was designed to measure the solids downflow flux at four points in the cross-sectional area of the downer, as shown in Figure 2. These four measured points are located at the same elevation of the downer and at the same radial position. As shown in Figure 3, the solids downflow flux can be considered to be axially symmetric after the solids entrance region.

In the tracing technique, helium was chosen as a tracer in order to eliminate the effect of gas adsorption on catalyst. A steady stream of tracer gas was injected by a probe on the axis of the bed at one elevation. The injection could be considered as a point source since the probe ended in a porous cylinder from which helium entered the bed in both the radial and the axial flow directions. During the measurements, the injected helium flow rate was about a half of the gas superficial velocity multiplied by the cross-sectional area of the porous plug. The helium flow rate was varied to demonstrate the low sensitivity of the measurements to the helium flow rate, as also shown by Li and Weinstein (1989). Samples were taken at three elevations ($x = 0.3$ m, 0.76 m, 1.3 m) downstream below the injector plane and at two elevations ($x = -0.14$ m, -0.3 m) upstream above the injector plane. The sample gas and the reference air were drawn into an on-line GOWMAC thermal conductivity analyzer connected to a data acquisition system. The fluctuations in the signal from the GOWMAC were smoothed by averaging 4,096 readings at 100 Hz. It was shown that such a recording length is long enough to give reproducible data. The complete setup for the measurement is shown in Figure 4.

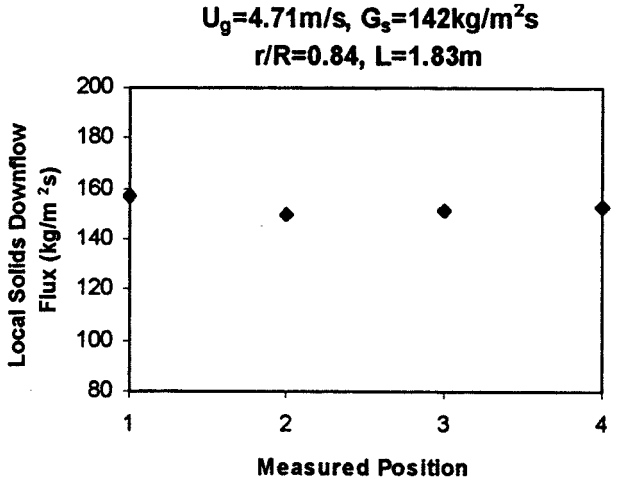

Figure 3. Demonstration of solids axial symmetry.

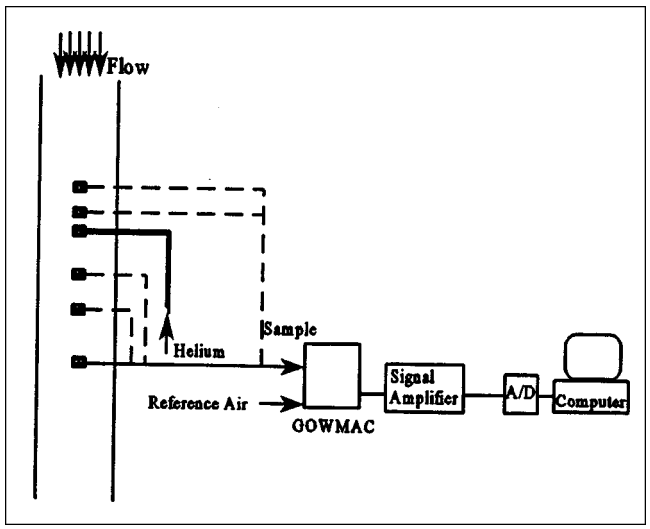

Figure 4. Experimental setup for helium tracing test.

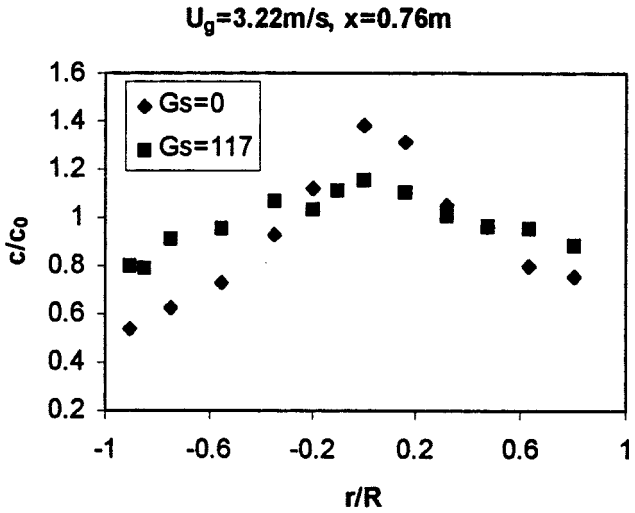

Figure 6. Effect of particles on the tracer profile.

Results and Discussion

The gas dispersion in a single-phase flow (gas) was investigated to provide the basis for comparing with that in two-phase flow. The profiles of the dimensionless helium concentration detected at several sampling locations are shown in Figure 5. The distribution of helium tends to be uniform when the sampling position is far from the injection source (1.3 m).

When solid circulation was added in the unit, the detected helium concentration distribution became significantly flatter in the column cross-sectional area than it is in one-phase flow, as shown in Figure 6. The reason is that the addition of solids to the gas flow enhances the turbulent mixing and results in greater lateral mixing.

Figure 7 shows the helium concentration profiles detected at three sampling distances between the tracer injector source and the sampling probe in the downer. It is obvious that the closer the sampling is to the injection, the more nonuniform the tracer distribution. A flat profile can be achieved at the location of about $x/D = 6$ or about 0.75 m.

The effect of solid circulation rate on the gas dispersion is illustrated in Figure 8. It is shown that the increase of solid rate at the same superficial gas velocity leads to more rapid gas lateral mixing. On the other hand, higher superficial gas velocity at the same solids circulation rate gives less rapid lateral mixing, as shown in Figure 9. Both effects are due to the fact that an increase of solid concentration in the downer provides better lateral mixing of the gas.

Figure 10 confirms the expected low backmixing in the downer. Due to the fact that the gas and particles are flowing downwards in the direction of gravity, convection is predominant over axial dispersion, and, therefore, backmixing detected upstream of the source is very limited. Only at a very close sampling distance between the injector and sampling probe planes and high helium injection rate, is there any detection of helium backmixing. In Figure 10, the backmixing level in the slow moving central core is surprisingly high and increases with increasing solid flux. In the gas only case, the backmixing level is lower, confirming that the presence of

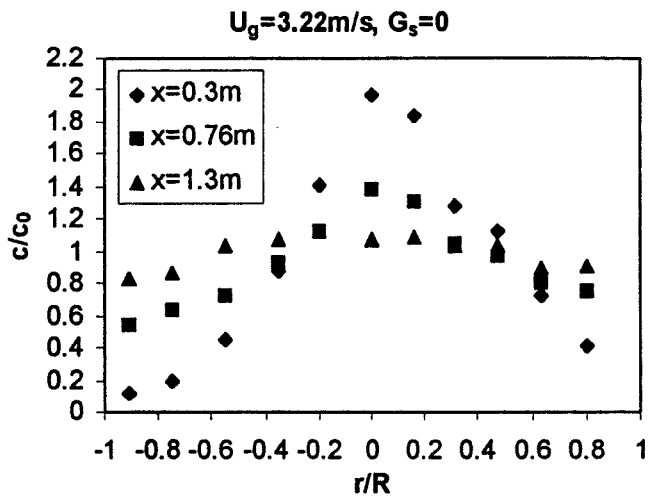

Figure 5. Gas dispersion in single (gas only) phase flow.

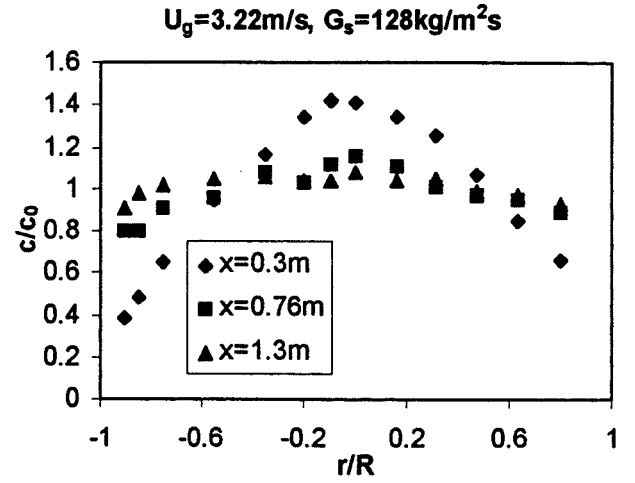

Figure 7. Profiles of dimensionless tracer concentration.

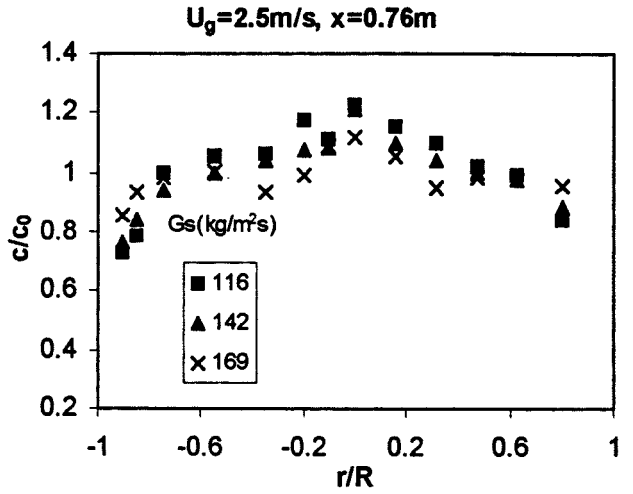

Figure 8. Effects of solids circulation rate on the gas dispersion.

solids enhances backmixing or axial dispersion. Also, the helium is readily detected both with and without solids present 14 cm above the injector, but is essentially undetectable 30 cm above. These data also confirm that the presence of solids enhance the turbulent mixing and indicate that the largest turbulent eddies with and without solids present are on the order of one to two tube diameters.

A two-dimensional, pseudo-homogenous model is used to describe the behavior of the gas dispersion in the downer. Assuming that isotropic dispersion takes place, this provides a dispersion coefficient independent of the local position in the column, which can be used with 1-D conversion models. Additional assumptions are that gas velocity is uniform in the column, and that convection occurs only in the axial direction. This is in keeping with 1-D modeling of the downer. In cylindrical coordinates, the model is formulated as follows

$$U\frac{\partial c}{\partial x} = D\left[\frac{1}{r}\frac{\partial}{\partial r}\left(r\frac{\partial c}{\partial r}\right) + \frac{\partial^2 c}{\partial x^2}\right] \tag{1}$$

with boundary conditions

$$\left.\frac{\partial c}{\partial r}\right|_{r=0} = 0$$
$$\left.\frac{\partial c}{\partial r}\right|_{r=R} = 0 \tag{2}$$
$$c(0,0) = c_0\,\delta(r,x)$$
$$c(r,-\infty) = 0$$

The solution of above equation is

$$\bar{c} = \frac{c}{c_0} = Pe\sum_{n=0}^{\infty}\frac{J_0(\eta\lambda_n)\,e^{-\xi/4[-Pe+\sqrt{Pe^2+16\lambda_n^2}]}}{J_0^2(\lambda_n)\sqrt{Pe^2+16\lambda_n^2}} \quad \text{when } \xi \geq 0 \tag{3a}$$

$$\bar{c} = \frac{c}{c_0} = Pe\sum_{n=0}^{\infty}\frac{J_0(\eta\lambda_n)\,e^{\xi/4[Pe+\sqrt{Pe^2+16\lambda_n^2}]}}{J_0^2(\lambda_n)\sqrt{Pe^2+16\lambda_n^2}} \quad \text{when } \xi \leq 0 \tag{3b}$$

where η and ξ are nondimensionlized coordinates

$$\eta = \frac{r}{R}$$
$$\xi = \frac{x}{R}$$

and Pe is the Peclet number

$$Pe = \frac{U(2R)}{D}$$

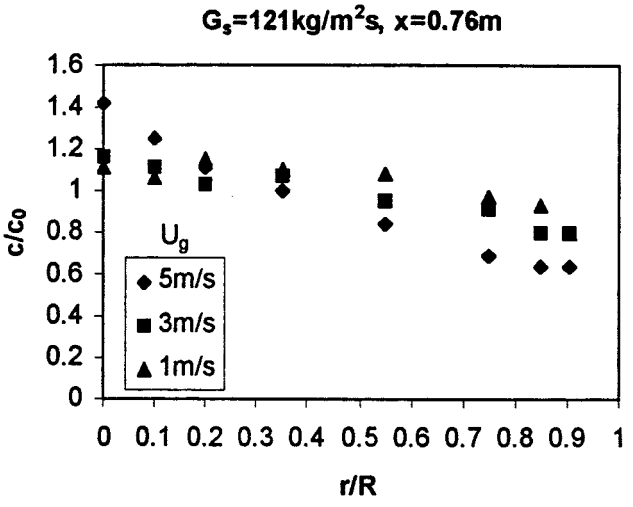

Figure 9. Effects of gas superficial velocity on the gas dispersion.

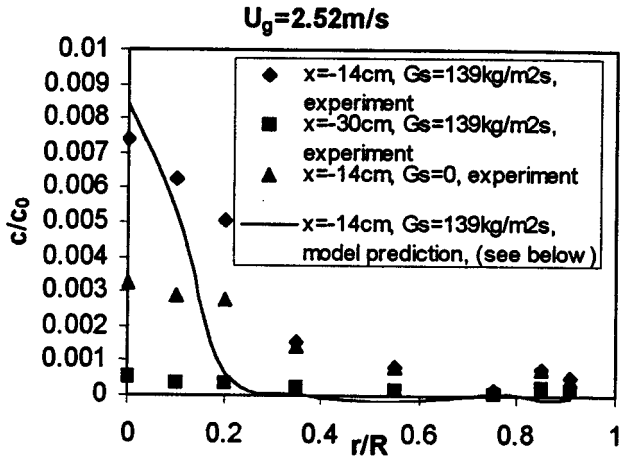

Figure 10. Gas backmixing in the downer.

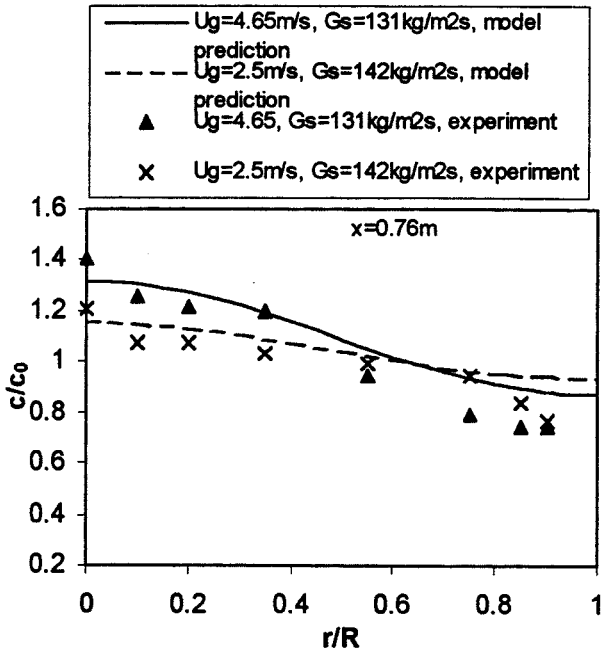

Figure 11. Comparison of the experimental results with the model predictions.

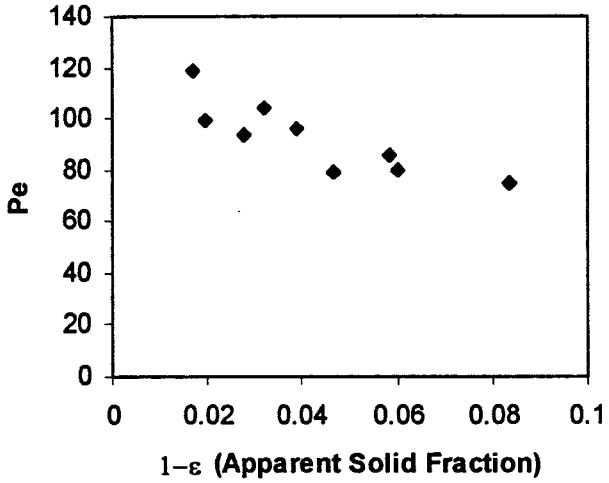

Figure 12. Estimation of the Peclet number.

λn is the root of the Bessel equation and can be obtained by solving $J_1(\lambda_n) = 0$.

Setting up the object

$$\sum_{\text{Minimum}} = \sum_{i=0}^{m} \left(\bar{c} - \bar{c}_{\text{experiment}}\right)^2 \qquad (4)$$

The model parameter *Pe* in the equation can be obtained by optimization. The results shown in Figure 11 indicate that the model prediction for the lateral mixing fits the experimental data well. The model prediction for the backmixing (see Figure10) shows good agreement with the experimental data as well. The average relative error is 5.4%. The deviation in the wall region is larger than in the core. The reason for this is that the model neglects the nonuniform radial distribution of gas velocity. The Peclet number of the two-phase flow in the downer is estimated from the above analysis. The variation of calculated Peclet number with the apparent solid fraction defined as $1 - \epsilon = (1/\rho_p g)(\Delta P/\Delta L)$ is plotted in Figure 12. It can be seen that the Peclet number decreases with increase of the bed density. This suggests that the particles reinforce the turbulent intensity of the flow.

The measured magnitude of gas dispersion coefficients are on the order of 10−100 cm^2/s, which agrees with the results obtained in the core region of the riser (Adams, 1988). The calculated Peclet number is on the order of 100, which agrees with the results obtained in a 6-in. downer-riser combination system (Zhu et al., 1995). The gas axial backmixing is much less than that in the riser. *This is its advantage:* the downer reactor can reduce gas backmixing over the riser, but keeps good lateral mixing.

Hydrodynamic studies (Cao, 1998; Zhu et al., 1995) in the downer have shown very significant differences in the gas-solid flow patterns between the downer and the riser. Gas tracer experiments (Weinstein et al., 1989; Cao, 1998; Li and Weinstein, 1989) have also demonstrated differences between the downer and the riser in mixing properties. Comparisons between the downer and a riser are made to evaluate the performance of the newly proposed downer reactor for short contact reactions.

It has been determined that gas backmixing in the riser is the result of spatially distributed heterogeneity (Li and Weinstein, 1989). Helium tracing tests (Weinstein et al., 1989; Li and Weinstein, 1989) show that the tracer concentration detected upstream near the wall is much higher than that in the dilute core region when the injector is located near the wall. On the other hand, injection in the core region produced a very low level of backmixed tracer concentration, and the circumferential mixing in the annular region was considerable. They concluded that the assumption of gas plug flow in the riser was inappropriate for the whole bed. The same gas tracing equipment was used to measure the gas backmixing in the downer, as was used in the riser (Weinstein et al., 1989; Li and Weinstein, 1989). A comparison is shown in Figure 13. The injection point in the riser is near the wall ($r/R = 0.89$), but at the center in the downer. Figure 13 clearly shows that true gas backmixing occurring from a reverse flow region near the wall is very limited or nonexistent in the downer compared to riser flow. It is even undetectable when the detector is located 30 cm away from the injector source in the downer. The large reduction of true gas backmixing in the downer offers the advantage of improving the selectivity and productivity over a riser in many short contact reaction processes. On the other hand, the local mixing with a scale of about a diameter provides good lateral mixing characterized by the Peclet number, which is comparable between the riser and the downer. As shown in Figure 14, dispersion coefficients obtained in a riser (Adams, 1988) are plotted with the data obtained in the downer of this investigation. It can be seen that the radial gas dispersion coefficients in the downer have the same order of magnitude as in the riser. This ensures the good gas-solids contact, which is required in catalytic and thermal processes.

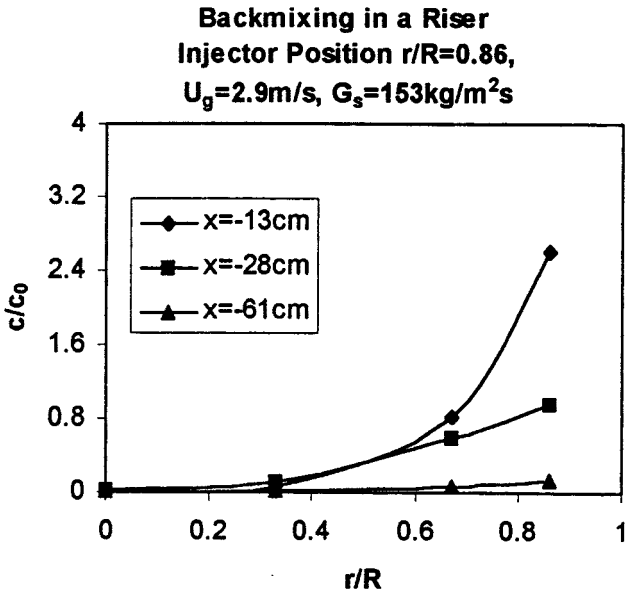

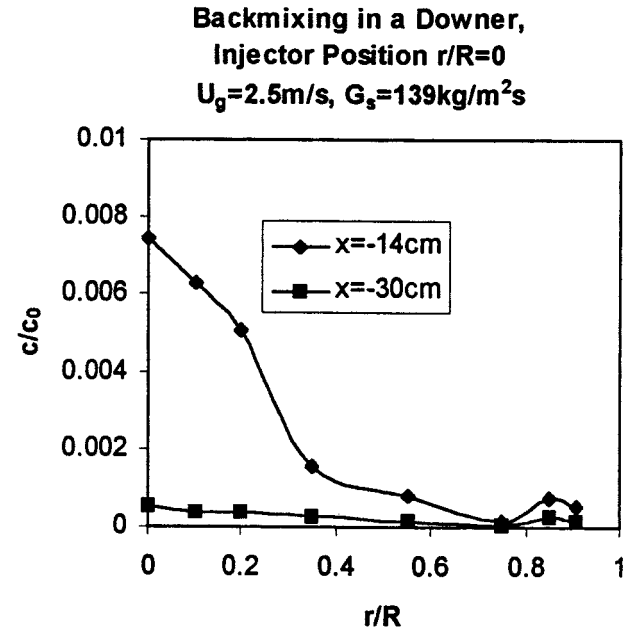

Figure 13. Comparison of gas backmixing between a downer and a riser.

Conclusion

Gas dispersion in the downer is affected by the solids density of the bed. Higher bed density results in more uniform lateral gas dispersion. Gas backmixing is very limited in downflowing high velocity fluidized beds. The lateral mixing is comparable with that in the riser.

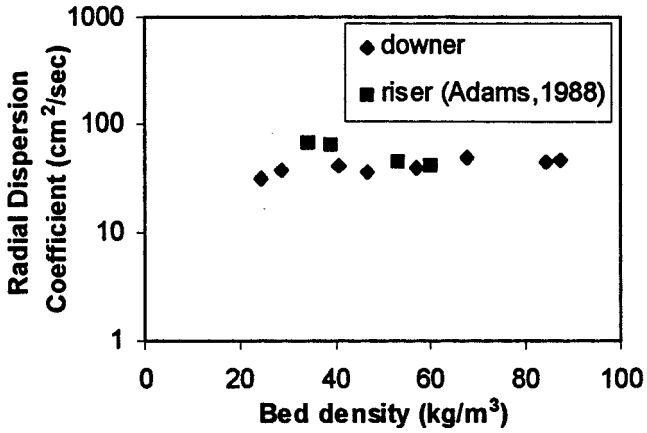

Figure 14. Comparison of gas lateral mixing between a downer and a riser.

Notation

c = measurement concentration, vol. %
c_0 = injection concentration, mean mixed vol. %
D = gas dispersion coefficient, m^2/s
ϵ = bed voidage
G_s = solids circulation rate, kg/m$^2\cdot$s
J_0, J_1 = Bessel functions
ΔL = distance between two pressure taps, m
ΔP = pressure difference, Pa
ρ_p = particle density, kg/m^3
r = radial coordinate, m
R = column radius, m
U_g = gas superficial velocity, m/s
U = gas velocity, m/s
x = distance between the injector and detector planes

Literature Cited

Adams, C. K., "Gas Mixing in a Fast Fluidized Bed," *Circulating Fluidization Technology II*, P. Basu and J. F. Large, eds., Pergamon Press, New York, p. 299 (1988).

Cao, C., "Characterization of Downflowing High Velocity Fluidized Beds," PhD Thesis, The City University of New York (1998).

Gartside, R. J., "QC—A New Reaction System," *Fluidization VI*, J. R. Grace, L. W. Shemilt, and M. A. Bergougnou, eds., Engineering Foundation, New York, p. 25 (1989).

Li, J., and H. Weinstein, "An Experimental Comparison of Gas Backmixing in Fluidized Beds across the Regime Spectrum," *Chem. Eng. Sci.*, **44**(8), 1697 (1989).

Murphy, J. R., "Evolutionary Design Changes Mark FCC Process," *Oil Gas J.*, **49** (May 18, 1992).

Schnitzlein, M. G., and H. Weinstein, "Flow Characterization in High Velocity Fluidized Beds Using Pressure Fluctuations," *Chem. Eng. Sci.*, **43**, 2605 (1988).

Weinstein, H., J. Li, E. Bandlamudi, H. J. Feindt, and R. Graff, "Gas Backmixing of Fluidized Beds in Different Regimes and Different Regions," *Fluidization VI*, J. R. Grace, L. W. Shemilt, and M. A. Bergougnou, eds., Engineering Foundation, New York, p. 57 (1989).

Zhu J. X., Z.Q. Yu, Y. Jin, J. R. Grace, and A. Issangya, "Cocurrent Downflow Circulating Fluidized Bed Reactors—A State of the Art Review," *Canadian J. of Chem. Eng.*, **73**, 662 (1995).

Manuscript received May 15, 1999, and revision received Nov. 1, 1999.